LncRNA TUG1 Knockdown Reduces Cardiomyocyte Damage in Viral Myocarditis by Targeting the miR-140-3p/CXCL8 Axis

ABSTRACT

Background: The purpose of this study was to probe the specific role of long noncoding RNA taurine up-regulation 1 (LncRNA TUG1) in viral myocarditis (VMC).

Methods: The mouse model of VMC was induced by Coxsackievirus type B3 (CVB3). LncRNA TUG1 was subsequently silenced, and micro-140-3p (miR-140-3p) was overexpressed in VMC mice. GenePharma synthesized wild-type and mutant LncRNA TUG1 or CXCL8 (C-X-C Motif Chemokine Ligand 8, Interleukin-8) fragments containing the miR-140-3p binding site and cloned them into the pmirGLO luciferase reporter vector. Dual luciferase reporter assays were performed to test the activity of LncRNA TUG1 or CXCL8 fragments containing miR-140-3p mimic and mimic NC. The effects of silencing LncRNA TUG1 on cell proliferation, apoptosis, and inflammation in the VMC mouse model and in vitro were investigated by flow cytometry, enzyme linked immunosorbent assay, and western blot.

Results: In the VMC mouse model, LncRNA TUG1 and CXCL8 were upregulated, while miR-140-3p was downregulated. Suppressing LncRNA TUG1 led to inhibition of CXCL8 by promoting miR-140-3p. Suppressing LncRNA TUG1 or CXCL8 or restoring miR-140-3p were observed to increase cell viability and decrease apoptosis rate of cardiomyocytes.

Conclusion: LncRNA TUG1 knockdown suppresses inflammation and damage of VMC cardiomyocytes via the miR-140-3p/CXCL8 axis.

Keywords: LncRNA TUG1, miR-140-3p, CXCL8, viral myocarditis

ORIGINAL INVESTIGATION

INTRODUCTION

Myocarditis (MC) is an inflammatory disease that has an incidence of less than 10% of the population.[1] Myocarditis is usually manifested by chest pain, palpitations, and breathing difficulties, and some cases may develop into heart failure.[2] Myocarditis is caused by a variety of infectious and non-infectious factors, myocardial inflammation, and damage.[3,4] Virus is widely regarded as a key pathogenic factor for MC, accounting for about 50%-70% of all cases.[5,6] The underlying mechanisms of viral myocarditis (VMC) are still only partially understood, and there are no specific drugs for treatment. Therefore, it is urgent to study the molecular pathogenesis of VMC and search for its potential targets to provide new strategies for the prevention or treatment of VMC.

Long noncoding RNAs (LncRNAs) are important regulatory molecules for gene expression in a variety of developmental processes and diseases. In previous studies, in vitro and in vivo experiments have shown that LncRNAs regulate the progression of CVB3-induced MC. Studies to improve high-throughput screening and LncRNA expression profiling could reveal the presence of aberrant LncRNA expression during cardiac remodeling processes.[7,8] Also, LncRNA can regulate the onset and development of viral infections and may be of great value in the diagnosis of cardiomyopathies.[9,10] The role of LncRNAs in myocardial diseases has also received increasing attention. Liu et al[11] used microarrays to analyze LncRNA expression in leukocyte samples from patients with acute fulminant VMC, in which the LncRNA taurine up-regulation 1 (TUG1) was found to be abnormally

Ji Shi (iD)

Qiyin Sun (iD)

Department of Cardiology, The First People's Hospital of Huzhou, Huzhou City, Zhejiang Province, China

Corresponding author:
Qiyin Sun
✉ QiyinSundr@outlook.com

highly expressed. LncRNA TUG1 was first identified as crucial in photoreceptor and retinal formation. LncRNA TUG1 has been shown to contribute to inflammatory responses in the liver, heart, and kidneys. Most previous studies have explored the promotional effects of LncRNA TUG1 on the proliferation and metastasis of tumor diseases, such as bladder uroepithelial carcinoma, and esophageal squamous cell carcinoma.[12,13] Although LncRNA TUG1 has been found to be abnormally expressed in cardiomyopathies, studies on the mechanisms involved are still lacking.

LncRNAs can act as competitive endogenous RNAs (ceRNAs) and are associated with a variety of biological processes and tumorigenesis by competing with the response elements of microRNAs (miRNAs) for binding to messenger RNAs (mRNAs), thereby regulating the expression levels of mRNAs.[14] microRNAs are a class of highly conserved noncoding RNAs that regulate gene expression by binding to targeted mRNAs or complementary sequences within the 3'-UTR of targeted binding mRNAs.[15] Previous studies have shown that miR-140-3p may be associated with osteoarthritis, liver fibrosis, and tumorigenesis.[16,17] However, controversy still surrounds the cardioprotective role of miR-140-3p. It has been reported that circulating miR-140-3p may be a valuable biomarker for coronary artery disease risk assessment.[18] Another piece of evidence suggests that lower miR-140-3p levels in patients with cardiovascular disease are negatively associated with the risk of cardiovascular events and mortality.[19] miR-140-3p upregulation significantly restores myocardial ischemia/reperfusion injury and enhances cardioprotection.[20] However, it is still unknown whether miR-140-3p is involved in the development of VMC.

C-X-C motif chemokine ligand 8 (CXCL8) is a predicted target protein of miR-140-3p. C-X-C motif chemokine ligand 8 is a multicellular chemokine that recruits neutrophils and other immune cells to the inflammatory region.[21] Abnormal regulation of CXCL8 has been implicated in inflammation-mediated diseases, including inflammatory bowel disease, rheumatoid arthritis, psoriasis, asthma, and cystic fibrosis.[22]

This study aimed to investigate the effect of LncRNA TUG1 on VMC by regulating the miR-140-3p/CXCL8 axis.

METHODS

Animal Treatment
Thirty-two male BALB/c mice (SPF grade, 4-6 weeks old, 18-22 g) were provided by Shanghai Lab. Animal Research Center (Shanghai, China). Coxsackievirus B3 (CVB3) (Nancy strain) was provided by the State Key Laboratory of Virology (Wuhan, China). The mice were placed in a well-ventilated stainless-steel lattice-roofed pathogen-free cage at room temperature on a light/dark cycle for 12 hours.

Lentiviral vectors were provided by GeneChem (Shanghai, China). All mice were randomly divided into 4 groups: Blank (untreated normal mice), VMC, VMC + sh-TUG1, and VMC + sh-NC, with 8 mice in each group.

Coxsackievirus B3 was subpassaged by Hela cells (ATCC number: CCL-2). Coxsackievirus B3 infection (10^3 PFU) was given by intraperitoneal injection, while 0.1 mL of normal saline was considered a control. The day of vaccinating CVB3 is defined as day 0. On days 1 and 3, mice were intraperitoneally injected with lentivirus at a dose of 5×10^4 gtu/mouse. On day 7, mice were injected intraperitoneally with chloral hydrate (10%, 4 mg/g) for anesthesia, fixed in the supine position, and euthanized by neck breaking. The heart tissues were collected, rapidly frozen, and kept at $-80°C$.

Cell Culture
Cardiomyocyte HL-1 cells (ATCC number: CRL-1446; ATCC, USA) were cultured in Dulbecco's modified eagle medium (DMEM) (ATCC) containing 10% FBS (Gibco, USA) and 1% penicillin/streptomycin (Beyotime, Shanghai, China) at 37°C and 5% CO_2. Cells were passed every 48 hours. The HL-1 cells were divided into 2 groups: the control group and the CBV3 group. The CBV3 group was CBV-infected HL-1 cells. Cardiomyocytes were infected with 10 MOI of CVB3 diluted with DMEM. After that, cells were further cultured for 48 hours. Control cells were treated in the same way without CVB3.

Cell Transfection
CXCL8 was overexpressed using pcDNA3.1 (Invitrogen, Thermo Fisher Scientific) to form CXCL8 overexpression plasmid (pcDNA3.1-CXCL8) and its negative control (pcDNA3.1). GenePharma (Shanghai, China) synthesized small interfering RNA (si-TUG1) and its negative control (si-NC), miR-140-3p mimic, miR-140-3p inhibitor, and negative controls (mimic NC; inhibitor NC). To achieve transfection, the above oligonucleotides and plasmids were transfected into HL-1 cells immediately using Lipofectamine 3000 (Invitrogen), according to Lipofectamine 3000 (Invitrogen), at 37°C, and the medium was changed 6 hours later. After 48 hours, cardiomyocytes were assayed for quantitative reverse transcription polymerase chain reaction (RT-qPCR) or western blot to verify the transfection efficiency.

Quantitative Reverse Transcription Polymerase Chain Reaction
Total RNA from mouse heart tissue and HL-1 cells was extracted by TRIzol™ Reagent (Sigma, USA) and then detected by microspectrophotometer (Thermo, USA). cDNA synthesis of miRNA was performed by miRNA reverse transcription kit (Takara, Japan), and that of mRNA and lncRNA by PrimeScript™ RT Reagent kit (Takara). The synthesized cDNA was mixed with SYBR ®Premix Ex Taq™ (Takara) and RT-qPCR was implemented using ABI Prism 7300 system (Applied Biosystems, USA). Polymerase chain reaction (PCR) was amplified by predenaturation 95°C for 10 minutes and 40

HIGHLIGHTS
- LncRNA TUG1 is highly expressed in viral myocarditis (VMC).
- LncRNA TUG1 knockdown improves VMC.
- LncRNA TUG1 negatively mediates miR-140-3p levels.
- LncRNA TUG1 is involved in VMC by regulating miR-140-3p.

cycles of 90°C (10 seconds), 60°C (20 seconds), and 72°C (30 seconds). Polymerase chain reaction primers were synthesized by Beijing Genomics Institute (Beijing, China) and the $2^{-\Delta\Delta CT}$ method calculated relative gene expression. Table 1 shows qPCR primers. RT-qPCR was performed in triplicate.

Hematoxylin and Eosin Staining
Formalin-fixed heart tissue was paraffin-embedded and sliced (5 μm). The slices were dewaxed and rehydrated, then stained with hematoxylin solution, and re-stained in eosin solution. Imaging was performed using a microscope (DS-Ri2, Nikon, Japan).

TUNEL Staining
Heart tissue sections were dewaxed and stained with terminal deoxynucleotidyl transferase dUTP nick end labeling (TUNEL) kit (Roche, CA, USA). Heart tissue sections were reacted with a TUNEL reaction mixture with terminal deoxynucleotide transferase at 37°C for 1 hour and stained with DAPI (Beyotime). Positive apoptotic cells were marked in green and all nuclei were marked in blue. The results were visualized in the DAB system (Solarbio, Beijing, China) and viewed under a microscope (DS-Ri2, Nikon).

Cell Proliferation Assay
The cell viability for HL-1 cell proliferation was measured by CCK-8 assay (Beyotime). Simply put, treated HL-1 cells were plated into 96-well plates for 24 hours, and CCK-8 solution was incubated at 10 μL/well at 37°C for 1 hour. Optical density values (450 nm) were recorded using a microplate reader.

Table 1. Primer Sequences

Gene		Primer sequence (5′-3′)
Rat: TUG1 (amplicon length: 150 bp) transcript ID: NR_130147.2	Forward primer	CAGAACTCTGGAGGTGGACG
	Reverse primer	AGTTTGCACTGAGGGTCTGG
Mut: TUG1(amplicon length:133 bp) transcript ID: NM_001396521.1	Forward primer	TGAAGCCCCCATTTGAGTCC
	Reverse primer	CACCCTTCAGGCACCCTATG
miR-140-3p	Forward primer	TACCACAGGGTAGAACCACGG
	Reverse primer	Reverse universal primer
CXCL8 (CXCL15)	Forward primer	CTAGGCATCTTCGTCCGTCC
	Reverse primer	CAGAAGCTTCATTGCCGGTG
GAPDH	Forward primer	TTTGGCATTGTGGAAGGGCT
	Reverse primer	GGAGTTGCTGTTGAAGTCGC
U6	Forward primer	CTCGCTTCGGCAGCACA
	Reverse primer	AACGCTTCACGAATTTGCGT

Flow Cytometry
FITC Annexin V Apoptosis Detection Kit (BD Biosciences, USA) detected HL-1 cell apoptosis. Treated HL-1 cells in the culture medium were obtained by centrifugation, rinsed with pre-cooled PBS (Beyotime), and resuspended in 500 μL 1× binding buffer, and incubated with Annexin V-FITC and PI away from light. BD FACSCanto II flow cytometry (BD Biosciences) was adopted for detection. There were 3 replicates for each group, and the experiments were repeated 3 times.

Enzyme Linked Immunosorbent Assay
HL-1 cell culture supernatant and mouse heart homogenate were collected. Interleukin-6 (IL-6), interleukin 1-beta (IL-β), and interferon-gamma (IFN-γ) were determined using enzyme linked immunosorbent assay (ELISA) kits (R&D Systems, USA). There were 3 replicates for each group, and the experiments were repeated 3 times.

Oxidative Stress Detection
DCFH-DA (C2938, Thermo Scientific), Lipid Peroxidation MDA Assay Kit (Beyotime), and Total Superoxide Dismutase Assay Kit with WST-8 (Beyotime) were employed to quantitatively determine reactive oxygen species (ROS), Malondialdehyde (MDA), and Superoxide Dismutase (SOD) in HL-1 cells and mouse heart tissue, respectively.

Western Blot Analysis
Mouse heart tissue and HL-1 cells were lysed with RIPA lysis buffer (Solarbio) and the obtained protein was quantified by a BCA kit (Thermo Fisher Scientific). Twelve percentage of SDS-PAGE separation gel and concentrate gel were prepared (Beyotime), and the protein concentration was adjusted to 30 μg with sample buffer (Beyotime). The protein was electroblotted on an electrophoretic apparatus (Bio-Rad, USA) at 80 V for 40 minutes and 120 V for 2 hours, covered with PVDF membrane (Beyotime) at 200 mA for 2 hours, and blocked with TBST (Beyotime) containing 5% skim milk powder for 1 hour. Next, primary antibodies were incubated at 4°C overnight, including p65 (ab32536, Abcam), p-p65 (3031, Cell Signaling Technology), CXCL8 (ab7747, Abcam), Bax (2272, Cell Signaling Technology), Cleaved Caspase-3 (9661, Cell Signaling Technology), Bcl-2 (ab196495, Abcam), and GADPH (5174, Cell Signaling Technology). The secondary antibody was incubated for 2 hours and developed with ECL solution (Beyotime) in a chemiluminescence imager (Image Quant LAS4000 mini, GE Healthcare). Image J software was utilized for gray analysis.

Luciferase Reporter Gene Assay
starBase 3.0 (http://starbase.sysu.edu.cn/) found binding sites between miR-140-3p and LncRNA TUG1 or CXCL8, and whether miR-140-3p targets both TUG1 and CXCL8 mRNA. GenePharma synthesized wild-type and mutant LncRNA TUG1 or CXCL8 fragments containing miR-140-3p binding sites. Plasmids containing the luciferase reporter of wild-type (WT) or mutant (MUT) TUG1 were created in-house, and phRL-TK was used as an internal control (Promega, Madison, WI, USA). The predicted binding sequence from TUG1 and miR-140-3p mimic were co-transfected. The WT fragment

of the CXCL8 3'-UTR containing the miR-140-3p binding site (WT-CXCL8) and the corresponding MUT fragment (MUT-CXCL8) were inserted into the pGL3 plasmid vector to generate a CXCL8 3'-UTR luciferase reporter gene construct. The synthesized products were cloned into the luciferase reporter vector to obtain WT-LncRNA TUG1 and MUT-LncRNA TUG1, and WT-CXCL8 and MUT-CXCL8, respectively. HL-1 cells were co-transfected with luciferase reporters and miR-140-3p mimic or mimic NC based on Lipofectamine®3000 (Invitrogen) and routinely cultured for 48 hours. Luciferase activity was measured using a dual luciferase reporter gene assay system (Promega) and Synergy 2 Multidetector Microplate Reader (BioTek Instruments Inc., USA).

RNA Pull-Down
RNA pull-down assay was carried out with an RNA pull-down kit (Pierce, Thermo Fisher Scientific). WT-TUG1 and MUT-TUG1 were labeled and purified using an RNA 3 terminal dethiobiotinization kit (Pierce). After PCR amplification and digestion of the DNA fragments of WT-TUG1 or MUT-TUG1, biotin RNA was used to label WT-TUG1 and MUT-TUG1, which were named Bio-TUG1 WT and Bio-TUG1 MUT, respectively, and Bio-NC was used as a control. Biotinized (Bio)-TUG1 WT and Bio-TUG1 MUT were coupled to streptavidin beads. After lysis, RNA complexes were obtained and purified with TRIzol reagent (Sigma-Aldrich) to determine miR-140-3p by RT-qPCR.

Data Analysis
All data were analyzed using Granpad Prism 8 and expressed as mean ± standard deviation (SD). All experiments were biologically replicated at least 3 times. Two-group datasets were analyzed by Student's *t*-test or Mann—Whitney *U* test, and multiple-group datasets by one-way analysis of variance. *P < .05 outlined statistical significance. Supplementary Table 1 shows all data.

Statement
No artificial intelligence (AI)—assisted technologies were used in the production of submitted work.

RESULTS

LncRNA TUG1 is Highly Expressed in Viral Myocarditis
After CVB3 injection, pathological changes in heart tissue were observed by hematoxylin and eosin (HE) staining. The heart tissue of VMC mice showed obvious symptoms of injury and inflammation (Figure 1A). TUNEL staining showed significantly more positive results in the heart tissue in VMC mice than in untreated normal mice (Figure 1B). CCK-8 assay and flow cytometry showed a 54% decrease in cell proliferation and a 30.3% increase in apoptosis after infection with CVB3 (Figure 1C and D). At the same time, ROS and MDA contents increased and SOD contents decreased in the heart tissue of VMC mice and infected HL-1 cells (Figure 1E and F). Moreover, ELISA results showed that the heart tissue of VMC mice and HL-1 cells infected with CBV3 had increased contents of IFN-γ, IL-6, and IL-1β (Figure 1G and H). Western blot results showed forced levels of p65, p-p65, Bax, and Cleaved Caspase-3, and reduced levels of Bcl-2 in cardiac tissue of VMC mice and in CBV-infected HL-1 cells (Figure 1I-L).

Quantitative reverse transcription polymerase chain reaction results showed that LncRNA TUG1 levels in the heart tissue of VMC mice and infected HL-1 cells were promoted (Figure 1M and N).

LncRNA TUG1 Knockdown Improves Viral Myocarditis
To determine the biological function of LncRNA TUG1 in VMC mice and cardiomyocytes, LncRNA TUG1 shRNA and siRNA were utilized to knock down LncRNA TUG1 in VMC mice and cardiomyocytes, respectively. Quantitative reverse transcription polymerase chain reaction showed that LncRNA TUG1 expression in VMC mice and VMC cells was reduced after LncRNA TUG1 knockdown (Figure 2A and B). Hematoxylin and eosin staining showed that VMC in mice was improved after LncRNA TUG1 knockdown (Figure 2C). TUNEL staining showed that LncRNA TUG1 knockdown significantly reduced apoptotic cells in VMC mice heart tissue (Figure 2D). LncRNA TUG1 knockdown reduced IFN-γ, IL-6, IL-1β, p65, p-p65, Bax, and Cleaved Caspase-3 in the heart tissue of VMC mice (Figure 2E and F) and elevated Bcl-2 (Figure 2G). Meanwhile, ROS and MDA contents were suppressed, and SOD activity was activated (Figure 2H).

In VMC cells, VMC cell proliferation more than doubled, and apoptosis was alleviated, decreasing by 19.3% after LncRNA TUG1 knockdown (Figure 2I and J). In vitro ELISA and western blot results were consistent with in vivo results (Figure 2K-N).

LncRNA TUG1 Negatively Mediates miR-140-3p Levels
StarBase predicted miR-140-3p as the target of LncRNA TUG1 (Figure 3A). miR-140-3p in the heart tissue of VMC mice and infected HL-1 cells was kept at a relatively low level (Figure 3B and C). RNA pull-down and dual luciferase reporter gene assay verified the targeting relationship between LncRNA TUG1 and miR-140-3p, as reflected by that miR-140-3p was pulled down by Bio-TUG1 WT but not bio-TUG1 MUT (Figure 3D), and that the luciferase activity of HL-1 cells co-transfected with WT-TUG1 and miR-140-3p mimic was inhibited (Figure 3E). Subsequently, the regulatory effect of LncRNA TUG1 on miR-140-3p was studied, showing that LncRNA TUG1 knockdown enhanced miR-140-3p expression in infected HL-1 cells (Figure 3F).

LncRNA TUG1 is Involved in Viral Myocarditis by Regulating miR-140-3p
To explore LncRNA TUG1 and miR-140-3p interaction in VMC, si-TUG1 and miR-140-3p inhibitor were co-transfected into VMC cells. It was observed that si-TUG1 downregulated LncRNA TUG1 and upregulated miR-140-3p (Figure 4A). After LncRNA TUG1 knockdown, cell proliferation was induced and apoptosis was hampered (Figure 4B and C). Moreover, LncRNA TUG1 knockdown reduced IL-1β, IL-6, IFN-γ, p65, p-p65, Bax, and Cleaved Caspase-3, elevated Bcl-2 (Figure 4D-F), and suppressed oxidative stress injury (Figure 4G). However, these effects were rescued after transfection with miR-140-3p inhibitor.

miR-140-3p Targets CXCL8
As predicted by starBase, CXCL8 was a target of miR-140-3p (Figure 5A). CXCL8 in the heart tissue and cells was

upregulated in the VMC setting (Figure 5B and C). Luciferase data showed that co-transfection of WT-CXCL8 with miR-140-3p mimic resulted in luciferase activity reduction of HL-1 cells (Figure 5D). It was further checked that CXCL8 levels decreased or increased in HL-1 cells infected with CVB3 after transfection with miR-140-3p mimic and miR-140-3p inhibitor, respectively (Figure 5E and F). On the other hand, si-TUG1 transfection suppressed CXCL8 levels (Figure 5G and H).

LncRNA TUG1 Influences Viral Myocarditis by Controlling miR-140-3p/CXCL8 Axis

si-TUG1 and pcDNA 3.1-CXCL8 were co-transfected into HL-1 cells, and RT-qPCR results showed that the inhibition effect of si-TUG1 on CXCL8 was reversed by pcDNA 3.1-CXCL8 (Figure 6A). Functional experiments showed that LncRNA TUG1 knockdown promoted proliferation and reduced apoptosis rate (Figure 6B and C), as well as inhibited IL-1β, IL-6, IFN-γ, p65, p-p65, Bax, and Cleaved Caspase-3 and elevated Bcl-2 expression (Figure 6D-F). Moreover, LncRNA TUG1 knockdown alleviated cellular oxidative stress

(Figure 6G). However, these effects were attenuated by CXCL8 overexpression.

DISCUSSION

Among many viruses that cause VMC, CVB3 is a common strain of VMC, and the pathogenesis of CVB3-induced VMC model consists of direct myocardial injury, in which the virus directly impedes the metabolism of the host cells and leads to cell death, and indirect myocardial injury, in which a large number of inflammatory factors mediated by the immune system contribute to myocardial injury.[23] Therefore, this model has been widely applied to study acute infection and the chronic immune phase of human VMC. However, despite extensive research, the pathogenesis of CVB3-induced MC remains unclear, with limited research and treatment options.

Noncoding RNAs play an important role in the viral invasion of the host and in the immune response induced by infection. LncRNAs are universally involved in the regulation of various
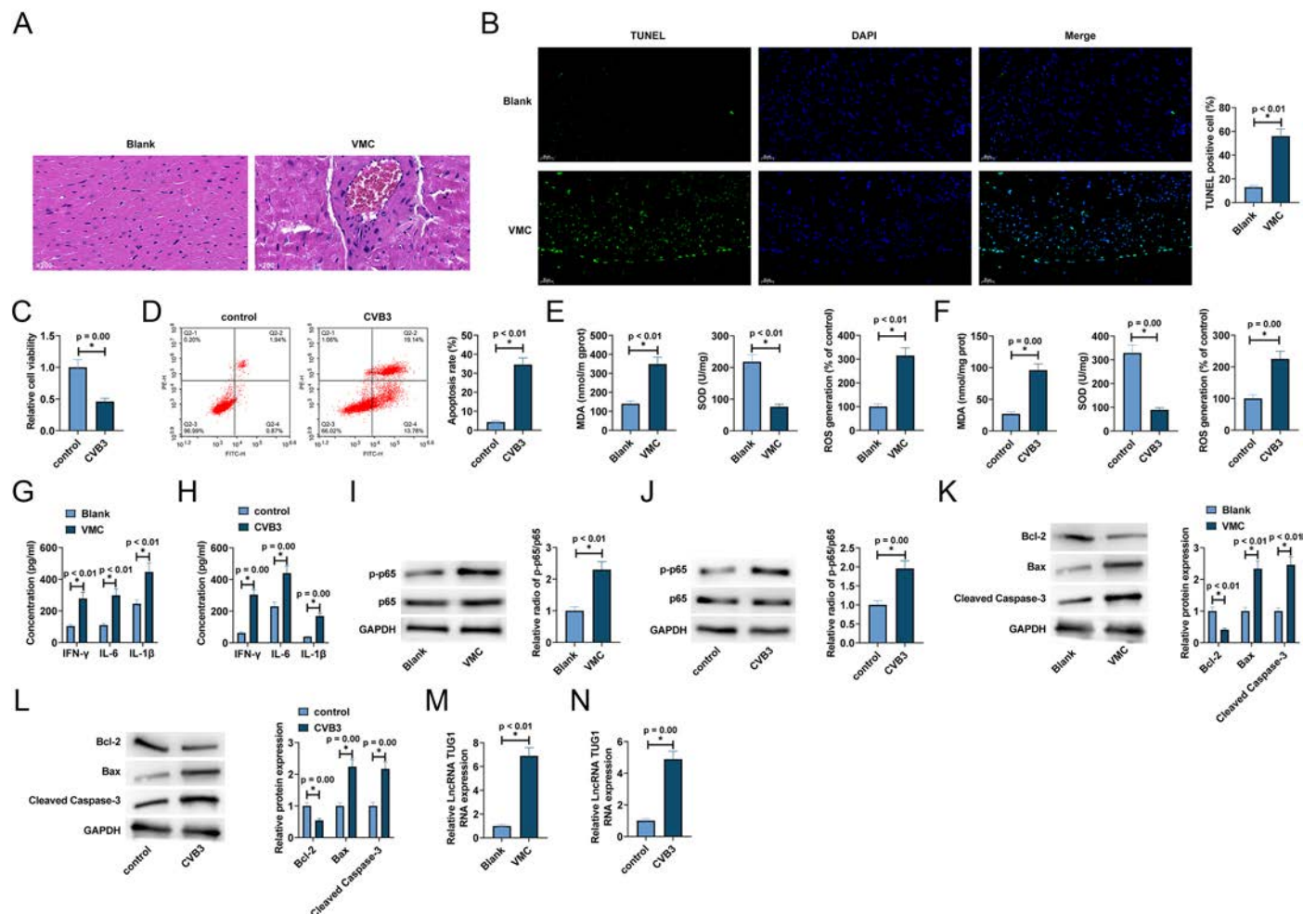

Figure 1. High expression of LncRNA TUG1 in VMC. A: HE staining of heart tissue (×200). B: TUNEL staining of heart tissue (×200). C: CCK-8 measured cell proliferation. D: Flow cytometry measured apoptosis rate. E, F: MDA, SOD, and ROS in heart tissue of mice and HL-1 cells. G, H: ELISA checked IFN-γ, IL-6, and IL-1β in mouse heart tissue and HL-1 cells. I, J: Western blot evaluated p65 and p-p65 in mouse heart tissue and HL-1 cells. K, L: Western blot evaluated Bcl-2, Bax, and Cleaved Caspase-3 in mouse heart tissue and HL-1 cells. M: RT-qPCR measured LncRNA TUG1 in heart tissue. N: RT-qPCR measured LncRNA TUG1 expression in HL-1. Data were expressed as mean ± SD (n = 3). *P < .05. *P < .05 vs. control mice.
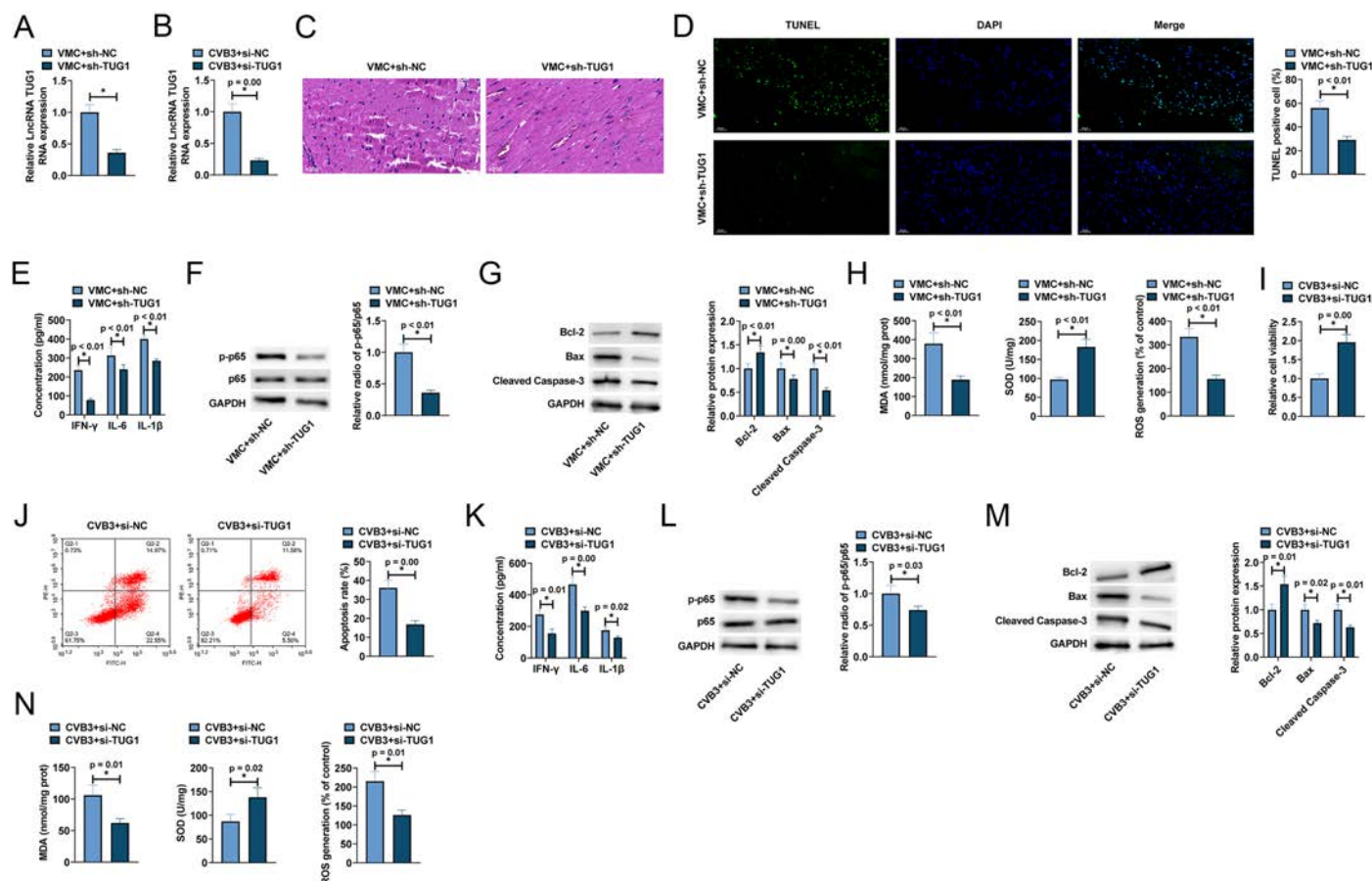
Figure 2. Silencing LncRNA TUG1 alleviates VMC. A, B: RT-qPCR measured LncRNA TUG1 expression in heart tissue and HL-1 cells after LncRNA TUG1 knockdown. C: HE staining of heart tissue (×200). D: TUNEL staining of heart tissue (×200). E: ELISA checked IFN-γ, IL-6, and IL-1β in mouse heart tissue. F: Western blot evaluated p65 and p-p65 in mouse heart tissue. G: Western blot evaluated Bcl-2, Bax, cleaved caspase-3 in mouse heart tissue. H: MDA, SOD, and ROS in heart tissue of mice. I: CCK-8 measured cell proliferation. J: Flow cytometry measured apoptosis rate. E, F: MDA, SOD, and ROS in heart tissue of mice and HL-1 cells. K: ELISA checked IFN-γ, IL-6, and IL-1β in HL-1 cells. L: Western blot evaluated p65 and p-p65 in HL-1 cells. M: Western blot evaluated Bcl-2, Bax, and Cleaved Caspase-3 in HL-1 cells. N: MDA, SOD, and ROS in HL-1 cells. Data were expressed as mean ± SD (n = 3). *P < .05. *P < .05 vs. control mice.

physiopathological processes such as cancer, tumorigenesis, immunity, inflammation, cell differentiation, and proliferation. Abnormally expressed LncRNAs were identified in the current study of the VMC model.[10] Given that some LncRNAs in the blood are highly stable and detectable and also have great potential in diagnosing MC. LncRNA TUG1 is a regulator present in a wide range of physiological or pathological processes, is ubiquitously expressed in vivo, and plays different roles in cancer, cardiovascular disease, neurological disease, digestive disease, and respiratory disease.[24] LncRNA TUG1 plays a crucial regulatory role in cardiovascular diseases, regulating atherosclerosis and myocardial fibrosis after myocardial infarction.[25] In this study, in vivo and in vitro models of VMC were used to mimic the pathogenesis, and the effects of LncRNA TUG1 on cardiomyocyte proliferation, apoptosis, and inflammatory responses in a model of VMC induced by CVB3 infection were explored by knocking down the expression of LncRNA TUG1. Interference with the expression of LncRNA TUG1 significantly improved the pathology of VMC mice, and the area of inflammatory

infiltration in cardiac tissues was reduced, attenuating apoptosis of cardiomyocytes in cardiac tissues, and reducing oxidative stress. Macrophage polarization plays a crucial role in regulating myocardial inflammation in CVB3-induced VMC.[26] Inhibition of CVB3 infection-induced activation of M1-type macrophages and promotion of macrophage polarization to M2-type can improve cardiac function in VMC, and IL-1β and IL-6 can be produced by macrophages and lymphocytes, which correlate positively with the degree of the body's inflammatory response.[27] The present study showed that serum IL-1β and IL-6 levels were significantly elevated in the VCM and CBV3 groups, suggesting the presence of inflammation in VCM mice and in HL-1 cells infected with CBV3. Taken together, these studies hypothesize that LncRNA TUG1 plays a proinflammatory role in VMC and affects the development of VMC.

At the transcriptional level, LncRNAs can further regulate the expression of mRNAs by competitively binding to miR-NAs, thereby affecting target proteins. This mechanism is currently the most widely studied in LncRNAs in various
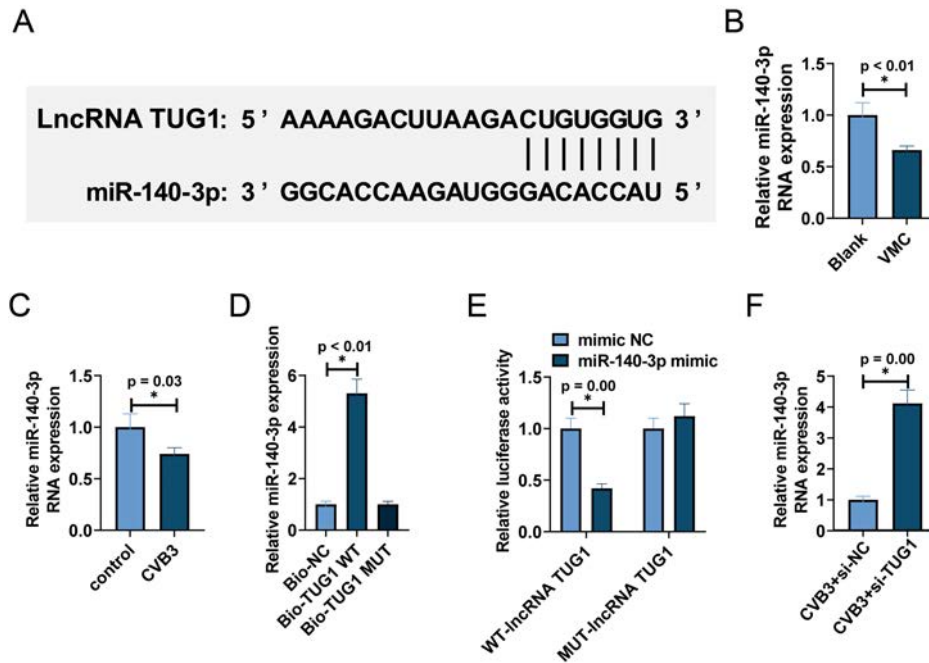
Figure 3. LncRNA TUG1 negatively regulates miR-140-3p expression. A: Binding sites between LncRNA TUG1 and miR-140-3p predicted by StarBase. B, C: RT-qPCR measured miR-140-3p in the myocardium of VMC mice. D, E: RNA pull-down and dual luciferase reporter assay measured the targeting relationship between LncRNA TUG1 and miR-140-3p. *$P < .05$ vs. NC mimic. F: RT-qPCR measured miR-140-3p in cells. Data were expressed as mean ± SD (n = 3). *$P < .05$.
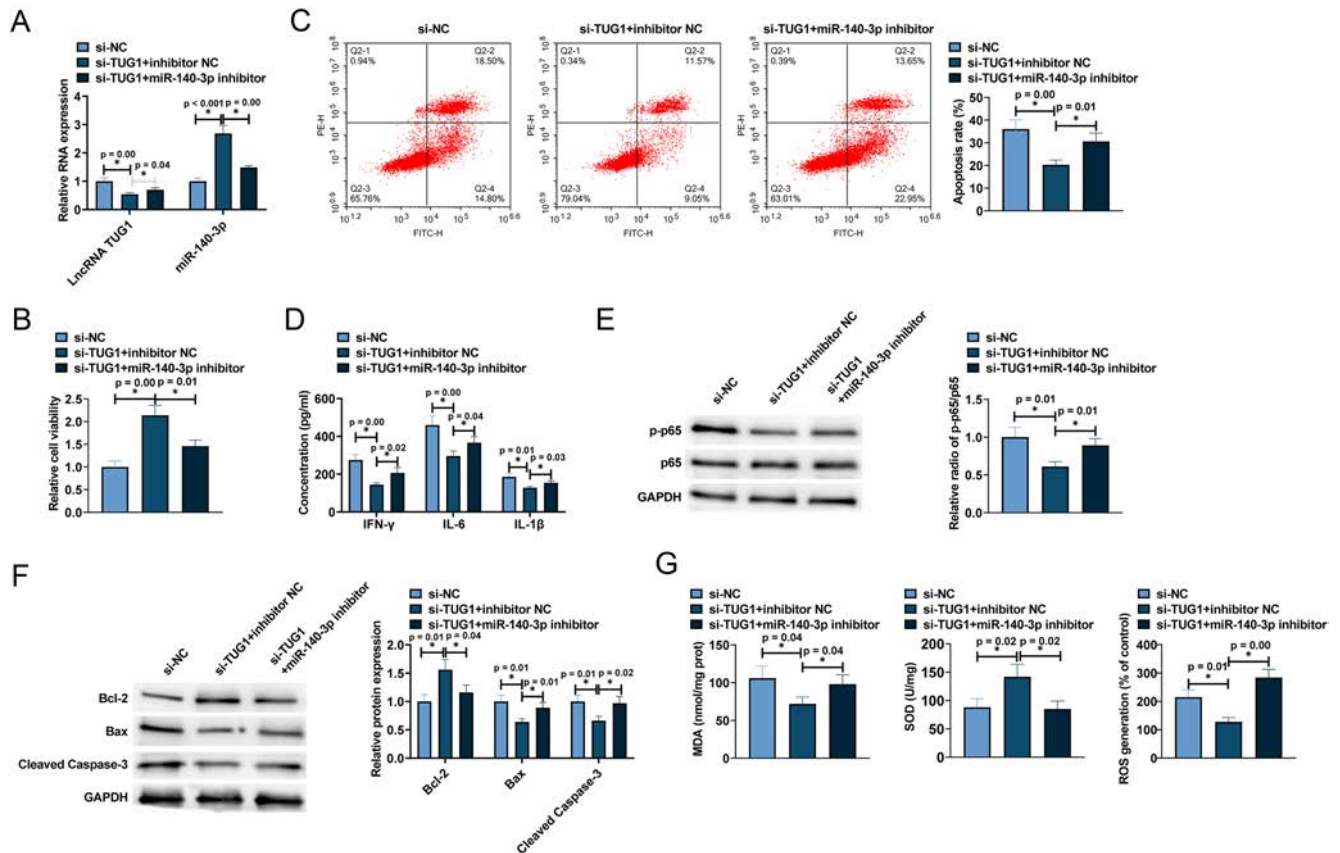

Figure 4. LncRNA TUG1 is involved in VMC by regulating miR-140-3p. A: RT-qPCR measured LncRNA TUG1 and miR-140-3p in VMC cells. B: CCK-8 measured cell proliferation. C: Flow cytometry measured apoptosis rate. D: ELISA checked IFN-γ, IL-6, and IL-1β in HL-1 cells. E: Western blot evaluated p65 and p-p65 in HL-1 cells. F: Western blot evaluated Bcl-2, Bax, and Cleaved Caspase-3 in HL-1 cells. G: MDA, SOD, and ROS in HL-1 cells. Data were expressed as mean ± SD (n = 3). *$P < .05$.
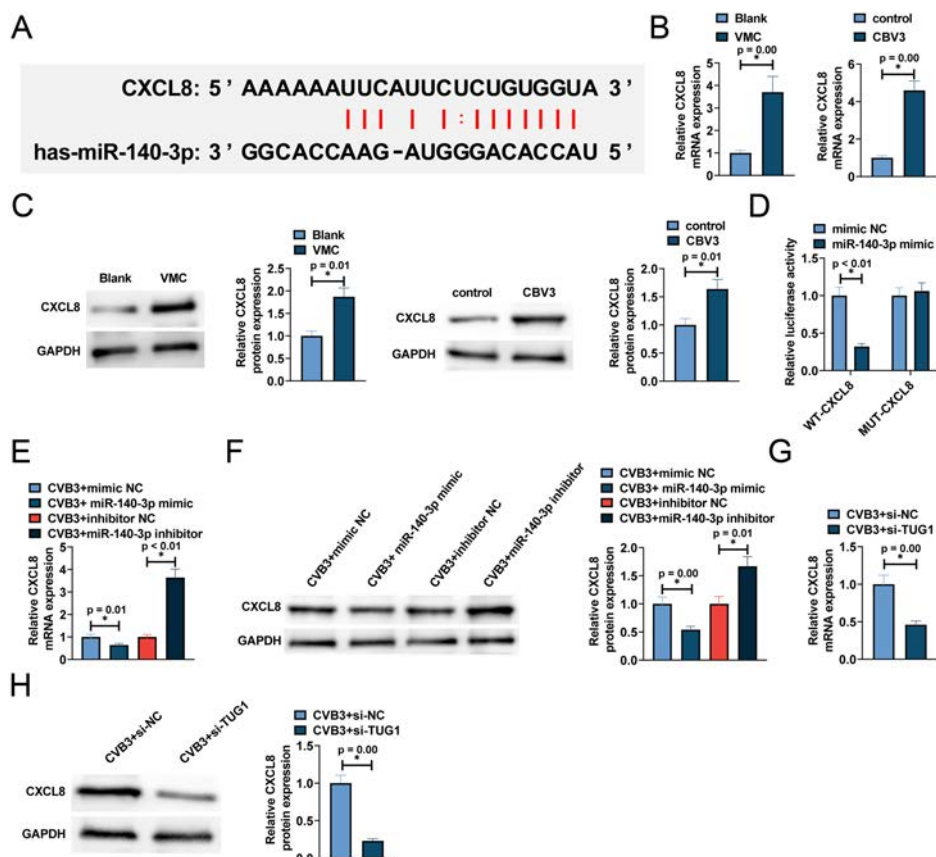
Figure 5. Knocking down LncRNA TUG1 can up-regulate the inhibition of CXCL8 expression by miR-140-3p. A: Binding sites between CXCL8 and miR-140-3p predicted by StarBase. B: RT-qPCR measured CXCL8 in mouse heart tissue and HL-1 cells. C: Western blot evaluated CXCL8 in mouse heart tissue and HL-1 cells. D: Targeting relationship between CXCL8 and miR-140-3p in the dual luciferase reporter gene assay. E, F: RT-qPCR detection and Western blot evaluated CXCL8 after altering miR-140-3p. G: RT-qPCR measured miR-140-3p and CXCL8 in cells after si-TUG1 treatment. H: Western blot evaluated CXCL8 after si-TUG1 treatment. Data were expressed as mean ± SD (n = 3). *P < .05.

diseases. miRNAs have been identified to play important roles in the regulation of various biological processes, including cell proliferation, apoptosis, and immune responses, and are involved in the regulation of vascular proliferation, cardiogenesis, heart failure, and cardiac hypertrophy.[28] LncRNA TUG1 and miR-140-3p interaction was confirmed, suggesting that LncRNA TUG1 negatively mediates miR-140-3p as a ceRNA. In addition, silencing miR-140-3p stimulated myocardial inflammation and injury in MC, but reducing miR-140-3p mitigated the decreased myocardial inflammation and injury in VMC cells induced by silencing LncRNA TUG1, which was characterized by an inflammatory response, oxidative stress, and apoptosis, and impaired proliferation. This is largely consistent with other previous miRNA regulatory mechanisms.[29] In virus-induced apoptosis, inhibition of miRNA expression largely reduces changes in the levels of apoptosis-associated proteins such as miR-34a and, in this study, miR-140-3p. In contrast, miRNAs such as miR-222 and miR-21, whose expression is upregulated in the CBV3-induced VMC model, act as anti-apoptotic factors.[10] This suggests that there is aberrant expression of miRNAs in VMC

and that the extent of VMC could be reduced in the future by targeting these miRNAs.

To date, 17 C-X-C chemokines have been identified in humans, most of which are associated with cardiovascular disease. Among them, CXCL8 is mainly found in macrophages, and it has been shown that CXCL8 promotes the development of atherosclerosis through macrophage recruitment.[30,31] Furthermore, it has been shown that CXCL8 induces inflammatory cell infiltration in infarcted myocardium and promotes myocardial infarction in the presence of myocardial ischemia.[32] These evidence suggest that CXCL8 is involved in the development of heart diseases. In addition to this, VMC is closely related to the immune response. Infiltration of immune cells usually leads to tissue injury. Injured tissues further release IFN-γ to promote T-lymphocyte migration. Injured tissues express CXCL8, which regulates neutrophil accumulation and promotes vascular inflammation, dysfunction, and injury.[33] This suggests that CXCL8 may play an important role in VMC. In this study, we confirmed that CXCL8 is a target mRNA of miR-140-3p.
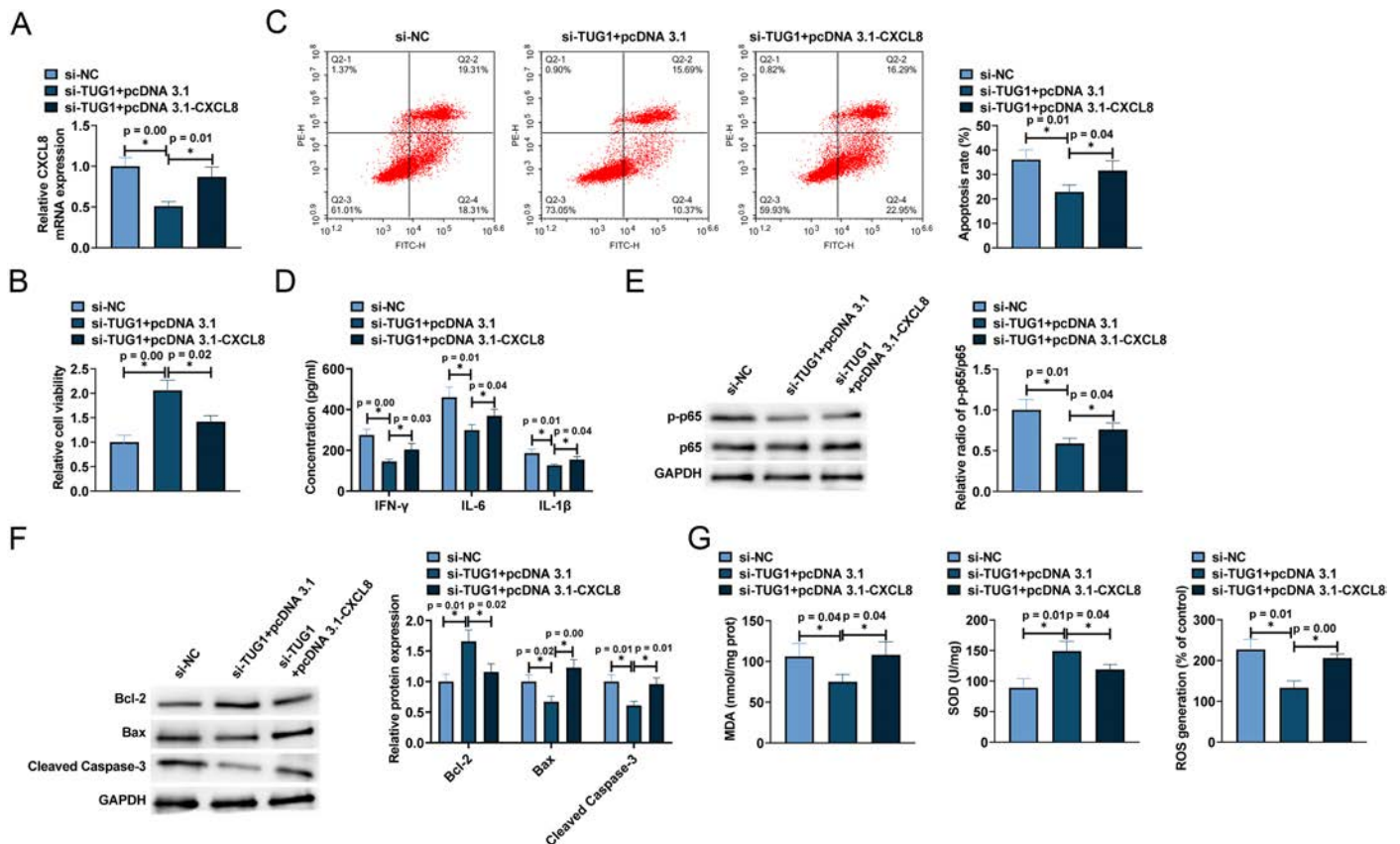
Figure 6. LncRNA TUG1 influences VMC by regulating the miR-140-3p/CXCL8 axis. A: RT-qPCR measured LncRNA TUG1 and CXCL8 in VMC cells. B: CCK-8 measured cell proliferation. C: Flow cytometry measured apoptosis rate. D: ELISA checked IFN-γ, IL-6, and IL-1β in HL-1 cells. E: Western blot evaluated p65 and p-p65 in HL-1 cells. F: Western blot evaluated Bcl-2, Bax, and Cleaved Caspase-3 in HL-1 cells. G: MDA, SOD, and ROS in HL-1 cells. Data were expressed as mean ± SD (n = 3). *P < .05.

In addition, CXCL8 expression was elevated in VMC tissues and CBV3-infected HL-1 cells, and restoring CXCL8 expression could counteract myocardial inflammation and injury reduced by silencing LncRNA TUG1 on VMC cells, which was characterized by increased inflammatory factors, oxidative stress, apoptosis, and suppressed cell viability.

The present study has some limitations. High expression of LncRNA TUG1 in cardiomyocytes is a damaging factor, and it is closely related to the development of inflammatory response and immune response. However, our study has some shortcomings at present. For the LncRNA TUG1/miR-140-3p/CXCL8 axis to modulate CVB3 infection-induced VMC, this effect does not necessarily translate into meaningful clinical benefits. Moreover, the complexity of the LncRNA/miRNA/mRNAs regulatory network necessitates further investigation of the role of LncRNA TUG1 in clinical practice and detailed physiological mechanisms.

Overall, our results show that high expression of LncRNA TUG1 is observed in VMC mice and cells, and LncRNA TUG1 can regulate CXCL8 by binding to miR-140-3p, and silencing LncRNA TUG1 downregulates CXCL8 by binding to miR-140-3p. This regulation reduces the inflammation and damage of cardiomyocytes, which provides a new idea for developing targeted therapy for VMC.

REFERENCES

1.   Basso C. Myocarditis. *N Engl J Med.* 2022;387(16):1488-1500. [CrossRef]

2. Olejniczak M, Schwartz M, Webber E, Shaffer A, Perry TE. Viral myocarditis-incidence, diagnosis and management. *J Cardiothorac Vasc Anesth*. 2020;34(6):1591-1601. [CrossRef]

3. Reyes MP, Lerner AM. Coxsackievirus myocarditis--with special reference to acute and chronic effects. *Prog Cardiovasc Dis*. 1985;27(6):373-394. [CrossRef]

4. Fairweather D, Rose NR. Coxsackievirus-induced myocarditis in mice: a model of autoimmune disease for studying immunotoxicity. *Methods*. 2007;41(1):118-122. [CrossRef]

5. Dominguez F, Kühl U, Pieske B, Garcia-Pavia P, Tschöpe C. Update on myocarditis and inflammatory cardiomyopathy: reemergence of endomyocardial biopsy. *Rev Esp Cardiol (Engl Ed)*. 2016;69(2):178-187. [CrossRef]

6. Leonard EG. Viral myocarditis. *Pediatr Infect Dis J*. 2004;23(7):665-666. [CrossRef]

7. Wang Z, Zhang XJ, Ji YX, et al. The long noncoding RNA Chaer defines an epigenetic checkpoint in cardiac hypertrophy. *Nat Med*. 2016;22(10):1131-1139. [CrossRef]

8. Viereck J, Kumarswamy R, Foinquinos A, et al. Long noncoding RNA Chast promotes cardiac remodeling. *Sci Transl Med*. 2016;8(326):326ra22. [CrossRef]

9. Chen L, Zhou Y, Li H. LncRNA, miRNA and lncRNA-miRNA interaction in viral infection. *Virus Res*. 2018;257:25-32. [CrossRef]

10. Zhang C, Xiong Y, Zeng L, et al. The role of non-coding RNAs in viral myocarditis. *Front Cell Infect Microbiol*. 2020;10:312. [CrossRef]

11. Liu Q, Kong Y, Han B, Jiang D, Jia H, Zhang L. Long non-coding RNA expression profile and functional analysis in children with acute fulminant myocarditis. *Front Pediatr*. 2019;7:283. [CrossRef]

12. Han Y, Liu Y, Gui Y, Cai Z. Long intergenic non-coding RNA TUG1 is overexpressed in urothelial carcinoma of the bladder. *J Surg Oncol*. 2013;107(5):555-559. [CrossRef]

13. Xu Y, Wang J, Qiu M, et al. Upregulation of the long noncoding RNA TUG1 promotes proliferation and migration of esophageal squamous cell carcinoma. *Tumour Biol*. 2015;36(3):1643-1651. [CrossRef]

14. Khashkhashi Moghadam S, Bakhshinejad B, Khalafizadeh A, Mahmud Hussen B, Babashah S. Non-coding RNA-associated competitive endogenous RNA regulatory networks: novel diagnostic and therapeutic opportunities for hepatocellular carcinoma. *J Cell Mol Med*. 2022;26(2):287-305. [CrossRef]

15. Bartel DP. MicroRNAs: genomics, biogenesis, mechanism, and function. *Cell*. 2004;116(2):281-297. [CrossRef]

16. Ntoumou E, Tzetis M, Braoudaki M, et al. Serum microRNA array analysis identifies miR-140-3p, miR-33b-3p and miR-671-3p as potential osteoarthritis biomarkers involved in metabolic processes. *Clin Epigenet*. 2017;9:127. [CrossRef]

17. Wu SM, Li TH, Yun H, Ai HW, Zhang KH. miR-140-3p knockdown suppresses cell proliferation and fibrogenesis in hepatic stellate cells via PTEN-mediated AKT/mTOR signaling. *Yonsei Med J*. 2019;60(6):561-569. [CrossRef]

18. Karakas M, Schulte C, Appelbaum S, et al. Circulating microRNAs strongly predict cardiovascular death in patients with coronary artery disease-results from the large AtheroGene study. *Eur Heart J*. 2017;38(7):516-523. [CrossRef]

19. Vavassori C, Cipriani E, Colombo GI. Circulating microRNAs as novel biomarkers in risk assessment and prognosis of coronary artery disease. *Eur Cardiol*. 2022;17:e06. [CrossRef]

20. Yang D, Wang M, Hu Z, et al. Extracorporeal cardiac shock wave-induced exosome derived from endothelial colony-forming cells carrying miR-140-3p alleviate cardiomyocyte hypoxia/reoxygenation injury via the PTEN/PI3K/AKT pathway. *Front Cell Dev Biol*. 2021;9:779936. [CrossRef]

21. Sokol CL, Luster AD. The chemokine system in innate immunity. *Cold Spring Harb Perspect Biol*. 2015;7(5):a016303. [CrossRef]

22. Cambier S, Gouwy M, Proost P. The chemokines CXCL8 and CXCL12: molecular and functional properties, role in disease and efforts towards pharmacological intervention. *Cell Mol Immunol*. 2023;20(3):217-251. [CrossRef]

23. Yip F, Lai B, Yang D. Role of coxsackievirus B3-induced immune responses in the transition from myocarditis to dilated cardiomyopathy and heart failure. *Int J Mol Sci*. 2023;24(9):7717. [CrossRef]

24. Tam C, Wong JH, Tsui SKW, Zuo T, Chan TF, Ng TB. LncRNAs with miRNAs in regulation of gastric, liver, and colorectal cancers: updates in recent years. *Appl Microbiol Biotechnol*. 2019;103(12):4649-4677. [CrossRef]

25. Haybar H, Sadati NS, Purrahman D, Mahmoudian-Sani MR, Saki N. lncRNA TUG1 as potential novel biomarker for prognosis of cardiovascular diseases. *Epigenomics*. 2023;15(23):1273-1290. [CrossRef]

26. Gou W, Zhang Z, Yang C, Li Y. MiR-223/Pknox1 axis protects mice from CVB3-induced viral myocarditis by modulating macrophage polarization. *Exp Cell Res*. 2018;366(1):41-48. [CrossRef]

27. Bao J, Sun T, Yue Y, Xiong S. Macrophage NLRP3 inflammasome activated by CVB3 capsid proteins contributes to the development of viral myocarditis. *Mol Immunol*. 2019;114:41-48. [CrossRef]

28. Lu P, Ding F, Xiang YK, Hao L, Zhao M. Noncoding RNAs in cardiac hypertrophy and heart failure. *Cells*. 2022;11(5):777. [CrossRef]

29. Marketou M, Kontaraki J, Patrianakos A, et al. Peripheral blood microRNAs as potential biomarkers of myocardial damage in acute viral myocarditis. *Genes*. 2021;12(3):420. [CrossRef]

30. Domschke G, Gleissner CA. CXCL4-induced macrophages in human atherosclerosis. *Cytokine*. 2019;122:154141. [CrossRef]

31. Apostolakis S, Spandidos D. Chemokines and atherosclerosis: focus on the CX3CL1/CX3CR1 pathway. *Acta Pharmacol Sin*. 2013;34(10):1251-1256. [CrossRef]

32. Lu X, Wang Z, Ye D, et al. The role of CXC chemokines in cardiovascular diseases. *Front Pharmacol*. 2021;12:765768. [CrossRef]

33. Wang J. Neutrophils in tissue injury and repair. *Cell Tissue Res*. 2018;371(3):531-539. [CrossRef]

Supplementary Table 1. Experimental Results Data

Figure 1	Group		P
	Blank (n = 8)	VMC (n = 8)	
Figure 1B	13.00 ± 1.40	56.00 ± 6.00	<0.01
Figure 1E	140.00 ± 15.00	349.00 ± 36.00	< 0.01
	218.00 ± 22.00	76.00 ± 8.00	< 0.01
	100.00 ± 11.00	315.00 ± 32.00	< 0.01
Figure 1G	104.00 ± 11.00	278.00 ± 40.00	< 0.01
	110.00 ± 12.00	298.00 ± 40.00	< 0.01
	245.00 ± 25.00	446.00 ± 56.00	< 0.01
Figure 1I	1.00 ± 0.12	2.30 ± 0.30	< 0.01
Figure 1K	1.00 ± 0.13	0.41 ± 0.05	< 0.01
	1.00 ± 0.12	2.34 ± 0.24	< 0.01
	1.00 ± 0.10	2.46 ± 0.25	< 0.01
Figure 1M	1.00 ± 0.12	6.90 ± 0.70	< 0.01
	control	CVB3	
Figure 1C	1.00 ± 0.12	0.46 ± 0.05	0.00
Figure 1D	4.30 ± 0.70	34.60 ± 3.50	< 0.01
Figure 1F	27.00 ± 3.50	96.00 ± 10.00	0.00
	329.00 ± 33.60	89.00 ± 9.00	0.00
	100.00 ± 11.70	225.00 ± 24.00	0.00
Figure 1H	62.00 ± 7.00	304.00 ± 31.00	0.00
	230.00 ± 23.00	440.00 ± 46.00	0.00
	39.00 ± 4.00	169.00 ± 18.00	0.00
Figure 1J	1.00 ± 0.11	1.96 ± 0.20	0.00
Figure 1L	1.00 ± 0.10	0.54 ± 0.06	0.00
	1.00 ± 0.11	2.24 ± 0.23	0.00
	1.00 ± 0.12	2.17 ± 0.00	0.00
Figure 1N	1.00 ± 0.13	4.89 ± 0.50	0.00
Figure 2	**Group**		**P**
	VMC + sh-NC (n = 8)	VMC + sh-TUG1 (n = 8)	
Figure 2A	1.00 ± 0.12	0.36 ± 0.05	< 0.01
Figure 2D	56.00 ± 6.00	29.00 ± 3.00	< 0.01
Figure 2E	236.00 ± 24.00	78.00 ± 8.00	< 0.01
	313.00 ± 42.00	240.00 ± 25.00	< 0.01
	400.00 ± 20.00	285.00 ± 9.00	< 0.01
Figure 2F	1.00 ± 0.13	0.36 ± 0.04	< 0.01
Figure 2G	1.00 ± 0.11	1.34 ± 0.14	< 0.01
	1.00 ± 0.11	0.78 ± 0.08	0.00
	1.00 ± 0.10	0.54 ± 0.06	< 0.01
Figure 2H	379.00 ± 58.00	189.00 ± 20.00	< 0.01
	97.00 ± 6.00	183.00 ± 20.00	< 0.01
	334.00 ± 34.00	156.00 ± 16.00	< 0.01
	CVB3 + si-NC	CVB3 + si-TUG1	
Figure 2B	1.00 ± 0.13	0.23 ± 0.03	0.00
Figure 2I	1.00 ± 0.12	1.96 ± 0.20	0.00
Figure 2J	36.10 ± 4.00	16.80 ± 2.00	0.00
Figure 2K	275.00 ± 28.00	155.00 ± 29.00	0.01
	465.00 ± 47.00	299.00 ± 24.00	0.00
	175.00 ± 19.00	128.00 ± 10.00	0.02
Figure 2L	1.00 ± 0.13	0.74 ± 0.06	0.03

Supplementary Table 1. Experimental Results Data (*Continued*)

Figure 2M	1.00 ± 0.12	1.54 ± 0.17		0.01
	1.00 ± 0.11	0.72 ± 0.06		0.02
	1.00 ± 0.11	0.63 ± 0.05		0.01
Figure 2N	106.00 ± 16.00	62.00 ± 7.00		0.01
	87.00 ± 15.00	138.00 ± 20.00		0.02
	215.00 ± 26.00	126.00 ± 13.00		0.01
Figure 3		**Group**		**P**
	Blank (n = 8)	VMC (n = 8)	–	
Figure 3B	1.00 ± 0.12	0.66 ± 0.04	–	< 0.01
	Control	CVB3	–	
Figure 3C	1.00 ± 0.10	0.74 ± 0.06	–	0.03
Figure 3D	Bio-NC	Bio-TUG1 WT	Bio-TUG1 MUT	
	1.00 ± 0.10	5.30 ± 0.55	1.00 ± 0.11	< 0.01
Figure 3E	mimic NC	miR-140-3p mimic		
WT-lncRNA TUG1	1.00 ± 0.10	0.42 ± 0.05	–	0.00
MUT-lncRNA TUG1	1.00 ± 0.10	1.12 ± 0.12	–	0.25
Figure 3F	CVB3+si-NC	CVB3+si-TUG1	–	
	1.00 ± 0.10	4.12 ± 0.43	–	0.00
Figure 4		**Group**		
	si-NC	si-TUG1 + inhibitor NC	si-TUG1 + miR-140-3p inhibitor	'
Figure 4A	1.00 ± 0.12	0.54 ± 0.06[a]	0.70 ± 0.07[b]	
	1.00 ± 0.11	2.69 ± 0.28[a]	1.49 ± 0.06[a]	
Figure 4B	1.00 ± 0.13	2.14 ± 0.22[a]	1.26 ± 0.13[b]	
Figure 4C	36.10 ± 4.00	20.30 ± 2.10[a]	30.60 ± 3.70[b]	
Figure 4D	275.00 ± 28.00	144.00 ± 10.00[a]	206.00 ± 28.00[b]	
	460.00 ± 50.00	296.00 ± 26.00[a]	366.00 ± 32.00[b]	
	186.00 ± 19.00	128.00 ± 7.00[a]	154.00 ± 11.00[b]	
Figure 4E	1.00 ± 0.13	0.61 ± 0.07[a]	0.89 ± 0.09[b]	
Figure 4F	1.00 ± 0.12	1.56 ± 0.18[a]	1.16 ± 0.13[b]	
	1.00 ± 0.11	0.64 ± 0.06[a]	0.89 ± 0.09[b]	
	1.00 ± 0.11	0.66 ± 0.08[a]	0.97 ± 0.12[b]	
Figure 4G	106.00 ± 16.00	72.00 ± 9.00[a]	116.00 ± 12.50[b]	
	88.00 ± 15.00	142.00 ± 22.00[a]	91.00 ± 24.00[b]	
	215.00 ± 25.00	128.00 ± 15.00[a]	284.00 ± 29.00[b]	
Figure 5	**Group**			**P**
	Blank (n = 8)	VMC (n = 8)		
Figure 5B	1.00 ± 0.12	3.70 ± 0.70		0.00
Figure 5C	1.00 ± 0.11	1.87 ± 0.20		0.01
	control	CVB3		
Figure 5B	1.00 ± 0.11	4.60 ± 0.50		0.00
Figure 5C	1.00 ± 0.11	1.64 ± 0.17		0.01
Figure 5D	mimic NC	miR-140-3p mimic		
WT-CXCL8	1.00 ± 0.11	0.32 ± 0.04		< 0.01
MUT-CXCL8	1.00 ± 0.11	1.06 ± 0.11		
Figure 5E	CVB3 + mimic NC	CVB3 + miR-140-3p mimic		
	1.00 ± 0.12	0.64 ± 0.07		0.01
	CVB3 + inhibitor NC	CVB3 + miR-140-3p inhibitor		
	1.00 ± 0.11	3.64 ± 0.38		< 0.01

Supplementary Table 1. Experimental Results Data (*Continued*)

Figure 5F	CVB3 + mimic NC	CVB3 + miR-140-3p mimic	
	1.00 ± 0.12	0.54 ± 0.06	0.00
	CVB3 + inhibitor NC	CVB3 + miR-140-3p inhibitor	
	1.00 ± 0.13	1.67 ± 0.17	0.01
Figure 5G	CVB3 + si-NC	CVB3 + si-TUG1	
	1.00 ± 0.12	0.46 ± 0.05	0.00
Figure 5H	CVB3 + si-NC	CVB3 + si-TUG1	
	1.00 ± 0.11	0.23 ± 0.03	0.00

Figure 6		**Group**	
	si-NC	si-TUG1 + pcDNA3.1	si-TUG1 + pcDNA 3.1-CXCL8
Figure 6A	1.00 ± 0.11	0.51 ± 0.06[a]	0.87 ± 0.07[c]
Figure 6B	1.00 ± 0.14	2.06 ± 0.21[a]	1.52 ± 0.12[c]
Figure 6C	36.10 ± 4.00	22.90 ± 2.80[a]	31.60 ± 4.00[c]
Figure 6D	275.00 ± 28.00	145.00 ± 11.00[a]	206.00 ± 29.00[c]
	460.00 ± 50.00	299.00 ± 26.50[a]	326.00 ± 32.00[c]
	186.00 ± 19.00	126.00 ± 5.50[a]	154.00 ± 15.00[c]
Figure 6E	1.00 ± 0.13	0.59 ± 0.06[a]	0.76 ± 0.08[c]
Figure 6F	1.00 ± 0.12	1.66 ± 0.19[a]	1.16 ± 0.13[c]
	1.00 ± 0.11	0.67 ± 0.09[a]	1.28 ± 0.13[c]
	1.00 ± 0.11	0.61 ± 0.07[a]	0.96 ± 0.10[c]
Figure 6G	106.00 ± 16.00	75.00 ± 9.00[a]	108.00 ± 16.00[c]
	89.00 ± 15.00	149.00 ± 16.00[a]	119.00 ± 8.00[c]
	227.00 ± 25.00	128.00 ± 17.22[a]	206.00 ± 10.00[c]

[a]Compare with si-NC group; [b]Compare with si-TUG1+inhibitor NC group; [c]Compare with si-TUG1+pcDNA 3.1 group. CVB3, coxsackievirus B3; VMC, viral myocarditis.